

Fatigue fracture mechanisms and fractography of short-glassfibre-reinforced polyamide 6

J. J. HORST, J. L. SPOORMAKER

Laboratory for Mechanical Reliability, Industrial Design Engineering Department, Delft University of Technology Leeghwaterstraat 35, 2628 CB Delft, The Netherlands

An adaptation to existing failure models for fatigue fracture of short-fibre-reinforced thermoplastics is presented. This was based on results using some new experimental methods. These results led to the conclusion that cracks in glassfibre-reinforced polyamide 6 (conditioned to equilibrium water content) remain bridged by plastically drawn matrix material and/or fibres until just prior to final fracture. In this article, emphasis will be on the fractographic evidence for the existence of this failure mechanism. Also some other phenomena in glassfibre-reinforced polyamide will be mentioned. Apart from the normal fractographic investigations, specimens were cryogenically fractured after fatigue, revealing the structure of damage, before failure. Both fracture surfaces were compared, showing that only a small fraction of the fibres is broken in fatigue; mostly the fibres are pulled out. The mechanism consists of the following steps: damage begins with void formation, mainly at fibre ends; these voids coalesce into small cracks. These cracks, however, do not grow into one full crack, but the crack walls remain connected at several points. This is contrary to the fracture mechanism for the dry as-moulded material. When the material is dry as moulded, the matrix material cracks, without showing much ductility, and no bridges are formed.

Nomenclature

a	crack depth
K_I	stress intensity
K_{Ic}	critical stress intensity
N	number of cycles to failure
R	load ratio (minimum load divided by maximum load)
T_g	glass transition temperature
w	specimen width
Y	geometry factor
σ_{nom}	nominal stress

1. Introduction

Injection-moulded thermoplastics reinforced with short glass or carbon fibres are being used increasingly in load-bearing applications. Parts that were formerly made of metal are now being replaced by short-fibre-reinforced thermoplastics (SFRTPs) because of weight, cost, corrosion resistance and ease of production. This is by the injection-moulding process, which makes freedom of design and integration of functions possible. To be able to use the properties of this material fully, an extensive knowledge of the mechanical behaviour is needed.

A characteristic of SFRTPs is their high degree of anisotropy and inhomogeneity, caused by fibre orientation. Even simple geometries such as plates have different properties at different locations. In the product a layered structure is present [1–4]; generally skin,

shell and core layers are distinguished (Fig. 1). The fibre orientation in these layers is random, in the mould flow direction (MFD) and perpendicular to the MFD respectively. The orientations (average fibre direction and spread in orientation) in these layers as well as the thicknesses of the layers vary from location to location in the plate. Therefore the properties of the material vary throughout the plate. A consequence of this is that for example the tensile strength of specimens cut from an injection-moulded plate can vary between 100 and 160 MPa. This depends on the location from where the specimens were cut, and the direction of the axis of the specimen relative to the MFD. The modulus of elasticity of the specimens varies approximately to the same degree as the strength. These variations in properties occur in actual products. Also other features occur such as weld lines, shrinkage problems, and void formation at thick sections [5].

Our experiments [6–8] have shown that the fatigue strength (stress at which a certain fatigue lifetime is obtained) of glassfibre-reinforced polyamide (GFPA) specimens containing 30% glassfibres is directly proportional to the ultimate tensile strength (UTS), determined in a tensile experiment. In Fig. 2, Wöhler curves are shown for different specimen types. Normalization of the fatigue stress by the UTS of that specific specimen type leads to coincidence of the curves for the different specimens (Fig. 3), i.e., to a “master curve”. A similar relation between fatigue strength (in this case, the maximum stress intensity at

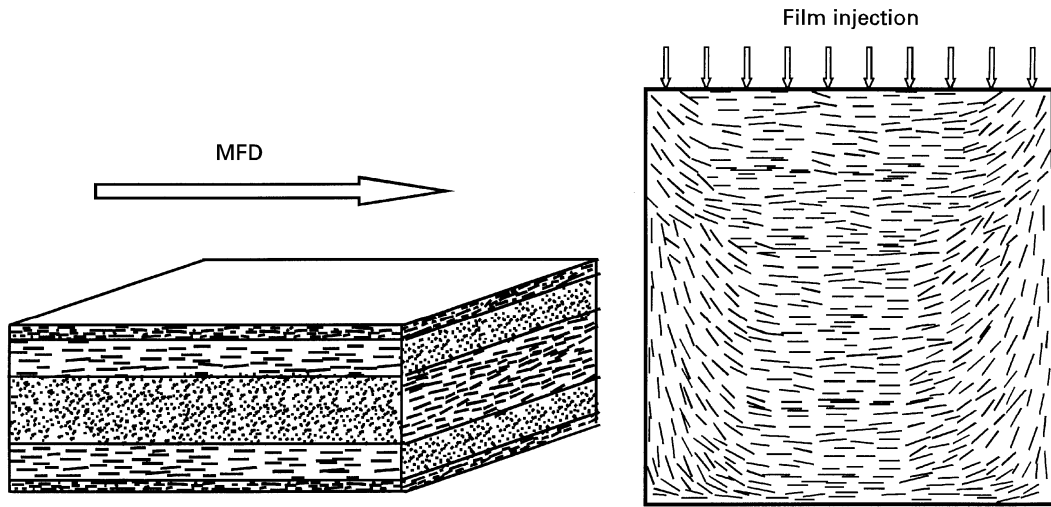


Figure 1 Schematic representation of fibre orientation in the specimen; three layers are distinguished (shown left). On the right the fibre orientation in the core layer of a square plate 6 mm thick is sketched.

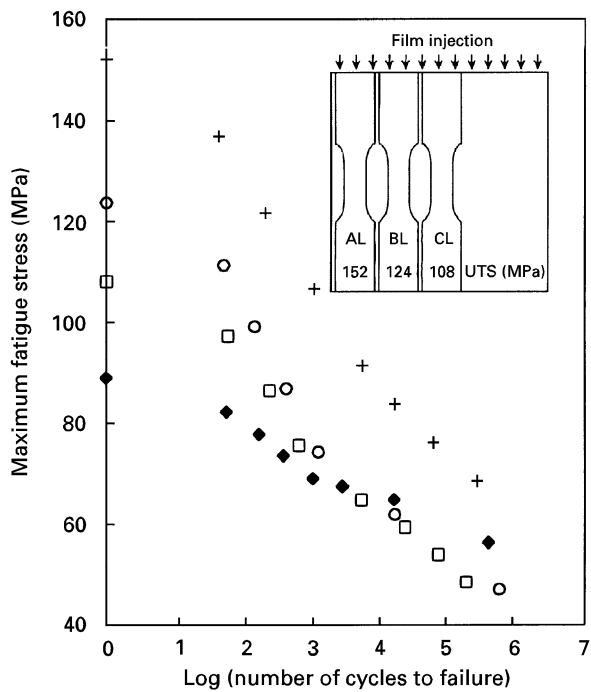


Figure 2 Wöhler curves for several specimen types. (○), BL type; (+), AL type; (□), CL type; (◆), PA unfilled. The value for log $N = 0$ is the UTS. The inset shows the locations of the specimens in the plate. For comparison also the values for non-reinforced PA are shown.

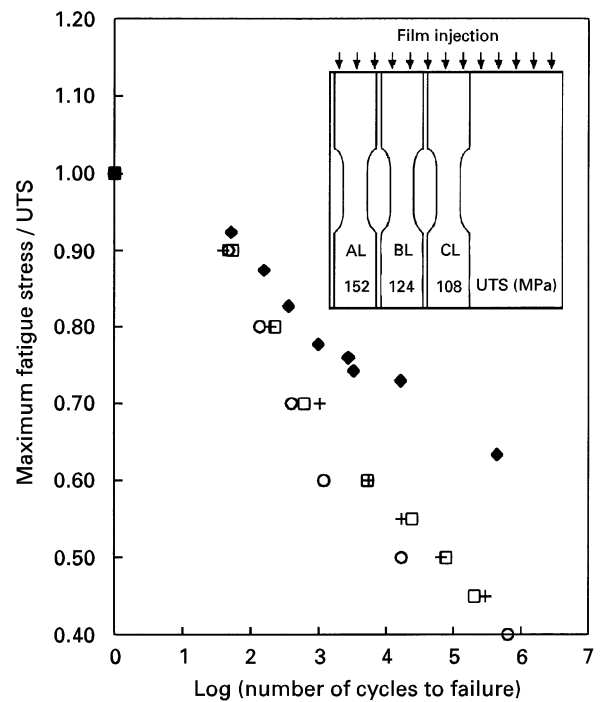


Figure 3 Normalized Wöhler curves for the same experiments as in Fig. 2. (○), BL type; (+), AL type; (□), CL type; (◆), PA unfilled. The maximum fatigue stress is divided by the UTS.

which a certain crack growth speed exists) and UTS was found for crack growth experiments [8].

The master curve has been found to change with various parameters [9]. These include conditioning of the specimens with respect to water content, average fibre length, test temperature and fibre–matrix bond quality.

A case for which the master curve is not valid is when a large proportion of the fibres have an orientation at an angle to the load direction (so they are neither parallel nor transverse), in particular the BL-type specimens 5.75 mm thick. These specimens show a fracture surface that is parallel to the major fibre

orientation and not perpendicular to the specimen axis, and a reduced fatigue strength (relative to the UTS). Obviously the mechanism in fatigue changes; the fibre–matrix interface is fatigued in a shear mode, which apparently leads to an early breakdown of interfacial strength, and early fracture.

The fatigue strength and the tensile strength (UTS) of a specimen are related. The fatigue and the tensile strength both depend in the same way on the orientation distribution inside the specimen. This is despite the different appearances of the fracture surfaces, and strongly different mechanisms in fatigue and tensile tests. For use of the “master curves” mentioned before in predicting the fatigue behaviour of structures,

knowledge of the conditions (temperature range, humidity, specimen thickness, fibre fraction and fibre aspect ratio) for which the master curves are valid is needed. The purpose of the current investigations is to understand the failure mechanism of the material and to explain why the master curve is valid. These can then be used in designing with greater confidence. This article focuses on the results of fractography, in obtaining insight in the mechanism.

2. Theory

2.1. Failure mechanism

Because of the complex structure of short-glassfibre-reinforced plastics, calculation of properties is much more complex than for continuously reinforced composites. However, methods for calculation of the elastic modulus have been successfully adapted for SFRTs [10–12], incorporating fibre length, fibre orientation and distribution of these. Also considerable success has been achieved in the calculation of strength [11] and impact strength or toughness [13]. However, for fatigue no calculation method is available, and we have to rely upon experimental data. To be able to apply experimental results with confidence, we have to understand the processes that occur during fatigue, and the implications thereof for the importance of the properties of the different elements for the fatigue behaviour. The three elements, fibre, matrix and fibre–matrix interface, all have their particular properties: strength, fatigue strength, elastic modulus, creep behaviour under cyclic loading, etc.

The mechanism in fatigue is often considered to consist of the following four stages [14].

1. Local weakenings due to cyclic deformation are initiated generally at the locations of highest stress intensity, the fibre ends [13].

2. Initiation of the crack occurs.

3. Crack growth takes place as a result of cyclic loading. Local modes of crack extension depend on the local fibre orientation, matrix ductility and the degree of interfacial adhesion [15]. The mechanisms during breakdown of the composite are fibre–matrix separation along the interfaces of fibres oriented parallel to the crack, deformation and fracture of the matrix between fibres, fibre pull-out, and fracture of transverse (to the crack direction) fibres [16].

4. Fast (instable) crack growth occurs in the last load cycle, which should be comparable with failure in a tensile test.

Hertzberg and Manson [17] reported that damage is initiated with debonding of fibres perpendicular to the load direction. Damage consequently grows into regions with fibre orientation at a smaller angle to the load.

Dally and Carrillo [18] reported for a system with the much more ductile polyethylene matrix an entirely different mechanism in fatigue. Massive debonding reduces the glass fibres from reinforcement to unbonded inclusions, giving rise to a sharp drop in the modulus. The greater strains are accommodated by the matrix without failure. This redistribution of strain causes the debonded region to enlarge progressively.

In measurements where the tensile strength of fatigued specimens (but not fatigued until failure) was determined, no decrease in strength could be found, in contrast with the PA 6 system.

This process of general degradation rather than a dominant crack was also reported by Mandell *et al.* [19] for unnotched specimens. Dibenedetto and Salee [20] observed a similar fatigue mechanism in compact tension specimens of graphite-fibre-reinforced PA 6.6, conditioned to equilibrium water content.

2.2. Scanning electron microscopy observations

2.2.1. Tensile experiments

Normally the fracture surface from a tensile experiment is reported to be microbrittle, except for materials with extremely ductile matrix material. This can be at high temperatures or high humidity (for PA), or for materials with exceptionally poor matrix-fibre bonding. Sato *et al.* [21] found for tensile fractured specimens a small ductile region in this brittle fracture surface. This ductile region is the initiation site for the crack. Sato *et al.* also performed *in-situ* experiments in the scanning electron microscope, revealing void formation and plastic deformation at the fibre ends, in PA 66 containing 30 wt% glassfibres.

2.2.2. Differences between fatigue and tensile experiments

Scanning electron microscopy (SEM) observations reported mainly by Lang *et al.* [15] show the following differences between fracture surfaces of glassfibre-filled PA 6.6 specimens broken in tensile and fatigue experiments.

1. More single- and multiple-fibre fracture in fatigue was seen, associated with buckling or bending of the fibres during crack closure.

2. Variations in interfacial failure site in well-bonded systems occurred. In tensile experiments the fibres remain covered with matrix material, while in fatigue the fibres generally do not show any sign of matrix material being still bonded to them. This shows the adverse effect of fatigue loading on interfacial bond strength.

3. Lang *et al.* [15] could not find any correlation between fracture surface characteristics and stress intensity difference ΔK or crack growth speed da/dn . Karger-Kocsis and Friedrich [22] reported, for GFPA 6.6, matrix ductility at high da/dn , due to hysteretic heating.

4. Lang *et al.* [15] also noted a difference in matrix behaviour between stable crack growth and fatigue crack propagation (FCP), with a higher matrix ductility in fatigue.

2.2.3. Fatigue experiments

Fractography of FCP fracture surfaces was done by various researchers [15, 23–28]. Generally the fracture surface appearance observed for the fatigue and the

final fracture area were similar to what was found by Lang *et al.* [15]. Both Karbhari and Dolgopolsky [23] and Karger-Kocsis and Friedrich [22] reported a variation in matrix ductility over the fatigue crack growth area. Brittle-like behaviour exists at the beginning of FCP, gradually becoming more ductile with ongoing crack growth. In the brittle fatigue area, very restricted pull-out was reported; in the ductile fatigue area, longer pull-out lengths exist. In this ductile zone the FCP rate decreases. Karbhari and Dolgopolsky [23] mentioned the following mechanisms: matrix pulling, fibre pull-out, crazing, shearing and fibre-induced matrix damage.

Lang *et al.* [15, 28] reported a dependence of the matrix ductility in FCP on fibre orientation, with more matrix ductility in the case of fibres perpendicular to the force. Also the fibre–matrix adhesion influences matrix ductility. Better adhesion puts a higher constraint on the matrix, leading to a local stress component perpendicular to the main stress direction. This enhances the severity of the local stress field, resulting in less matrix drawing.

2.3. Conclusions

The conclusions are that, although the mechanism in tensile experiments is clear, in fatigue two entirely different mechanisms were reported. One in which crack initiation and growth prevails, and another where a more general degradation takes place, without a crack being present.

Great differences exist in the degree of matrix ductility reported by different researchers. These differences are due especially to the matrix deformability, which for PA is very much dependent on the water content. Also the interface strength and fibre orientation must be considered to be important parameters, in determining which failure mechanism will prevail.

3. Experimental procedure

The material used was PA 6 containing 30 wt% glass-fibres (Akulon K224-G6, provided by DSM, The Netherlands). Square plates of dimensions 100 mm × 100 mm and 5.75 mm thickness were injection moulded from this. The mould was injected through a line gate, to obtain a straight flow front. For fatigue and tensile experiments, non-standard dogbone-type specimens were milled from the plates, using a Roland PNC-3000 computer-aided modelling machine. The location in the plate, the identification and the tensile strength of the types of specimen used are shown as insets in the graphs of the results.

The fatigue experiments were carried out on a servohydraulic MTS 810 bench. The load frequency used was 1 Hz, to avoid unacceptable temperature increase due to hysteretic heating and thermal failure of the specimen. Earlier experiments [8] showed the high sensitivity of the fatigue lifetime of this material to the test frequency. This is caused by hysteretic heating as a consequence of the high damping of the material. This is a consequence of the water absorption of the specimen, which lowers T_g to approximately ambient

temperature. During the experiments the temperature at the surface of the specimens was measured using an infrared contactless thermometer. The minimum-to-maximum-load ratio R was 0.1.

Tensile experiments were executed on the same type of specimens, with a cross-head speed of 50 mm min⁻¹, resulting in a nominal strain speed of 143% min⁻¹. Tests were carried out in an environmental chamber at a temperature of 23 °C and at a relative humidity (RH) of the air of 50%. Specimens had been conditioned by exposing them to laboratory air for at least 1 year, giving a water content of approximately 1.5%. Dry as-moulded specimens were stored in closed bags directly after injection moulding, and before testing these were stored in vacuum. Testing of these specimens took place at a low humidity (RH, 30–35%). No significant amount of water was absorbed during fatigue testing, which was checked by weighing the samples before and after the test.

Scanning electron micrographs of the fracture surface were made using a JEOL JSM-840A after gold coating of the fracture surfaces in a Balzers SCD 040. For some specimens the entire fracture surface was scanned, to enable us to calculate the area of the microductile and the microbrittle parts.

To reveal the structure inside the specimen while it is being fatigued, some specimens were first fatigued for a predetermined percentage of their lifetime and consequently fractured after immersion for 5 min in liquid nitrogen.

4. Results and discussion

As was shown in the previous sections, a profound knowledge of the fatigue mechanism is needed. This can be obtained partly by investigations during the fatigue experiment, e.g., the cyclic creep measurements presented in [6–8], but mostly by investigating closely the actual events that occur inside the material. On a macroscale, not much can be seen; the fracture surface in all cases appears to be brittle. It is sometimes very irregular, especially when the majority of fibres are oriented perpendicular to the fracture surface. Therefore we have to go to microscopic level, where the interactions between fibre and matrix can be observed. Fractography, especially using SEM is the most suitable method for observing the fracture surface, in particular because of the large depth of focus and high contrast.

4.1. Comparison of fatigued and tensile-tested specimens

For conditioned specimens, some clear differences could be observed between fracture surfaces of fatigued (Fig. 4) and tensile-tested specimens, respectively. Fig. 5 shows the final fast fracture for a fatigued specimen, similar to a tensile-tested specimen except for the shorter pull-out length.

The matrix ductilities for both cases are highly different. In the case of a *tensile-tested* specimen the fracture surface is microbrittle; sometimes a small area can be seen that is microductile, depending on the

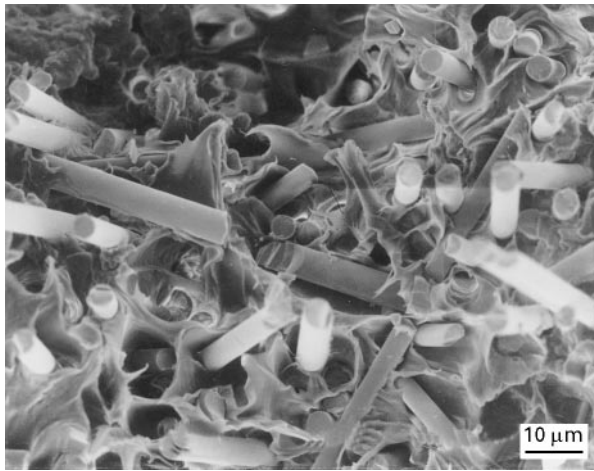


Figure 4 Representative fractograph of the fatigue part of the fracture surface of a fatigued specimen (conditioned AL-type specimen; fatigued at 45% of UTS; lifetime, 175.450 cycles).

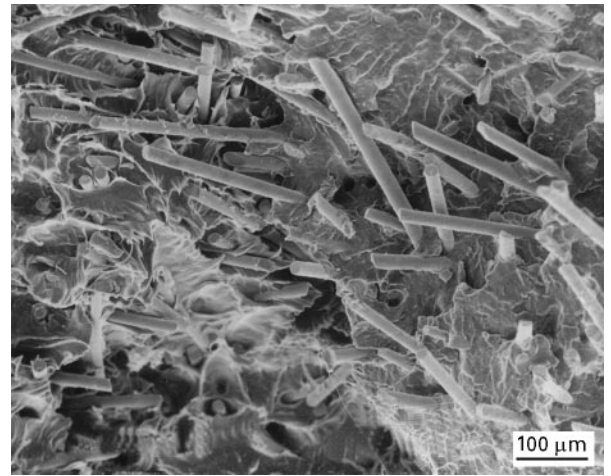


Figure 6 Fractograph of the transition between ductile and brittle part of the fracture surface of a fatigued specimen (conditioned AL-type specimen; fatigued at 45% of UTS; lifetime, 175.450 cycles).

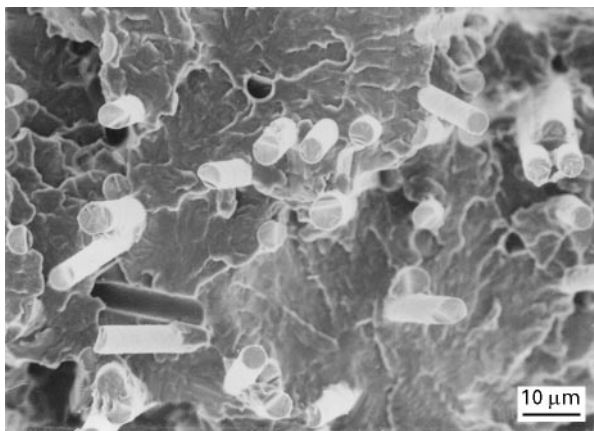


Figure 5 Representative fractograph of the final fast fracture part of the fracture surface of a fatigued specimen (conditioned AL-type specimen; fatigued at 45% of UTS; lifetime, 175.450 cycles).

amount of water absorbed. The ductile area can be 5–15% of the total fracture surface. This is the area where the crack is initiated, a slow process. When this crack dominates, the crack grows much more rapidly, not allowing the matrix material time to deform plastically. The fracture surfaces of the *fatigued specimens* show a much larger area with microductile behaviour, and a part with microbrittle behaviour. In Fig. 6 the transition from microductile to microbrittle fracture is shown. The size of the ductile area increases with decreasing maximum load in the fatigue experiment (see Section 4.3).

The fibre pull-out length is shorter (maximum, 50 μm) in both the microductile and the microbrittle part of the fatigued fracture surface, when compared with the fracture surface for the tensile test (pull-out length maximum, 150 μm). Generally this is ascribed to fibre buckling in the unloading part of the load cycle, where compressive forces act on the fibre when the “crack” closes. This cannot explain the short pull-out length in the microbrittle part of the fatigued fracture surface. The hypothesis for this shorter pull-

out length is that the crack growth speed for the final fracture area of the fatigued specimen is higher than in the tensile test. This higher speed leads to a shorter time for the fibres to be pulled out of the matrix, and a higher tendency to fracture of the fibres.

For the brittle part of the fracture surface of both tensile tests, as well as the fast fracture area of a fatigue test, matrix material can be seen adhering to the pulled-out fibres. In this case, it is not the interface that has failed but the matrix material some distance from the interface. Fibres in the microductile part of a fatigue test are completely clean, with no matrix material adhering to them. In fatigue the interface itself fails. We can conclude that the fatigue process has a detrimental effect on the fibre matrix bonding.

The conclusions are as follows.

1. The matrix material behaves in a more ductile manner in a fatigue test than in a tensile test. For the brittle areas no differences in matrix ductility could be observed for both cases.
2. The pull-out length in the fast fracture (brittle) area is longer in a tensile test than in a fatigue test.
3. The fibre–matrix bond in the fast fracture areas or tensile test is not broken, in contrast with the ductile (fatigue) areas.
4. The fibre–matrix bonding in the ductile areas seems to be better in a tensile test than in fatigue.

4.2. Comparison of conditioned and dry as-moulded specimens

Investigations were initiated using conditioned samples, as parts in service will generally be exposed to an atmosphere with RH between 30 and 70%. Large differences were found between these results using conditioned materials and the results in literature, where mostly dry as-moulded material was investigated. Therefore it was decided to compare the two materials: conditioned and dry as moulded.

Figs 7 and 8 show details of the fracture surface of a fatigued dry specimen, which can be compared with Figs 4 and 6 for the conditioned material. Conditioned

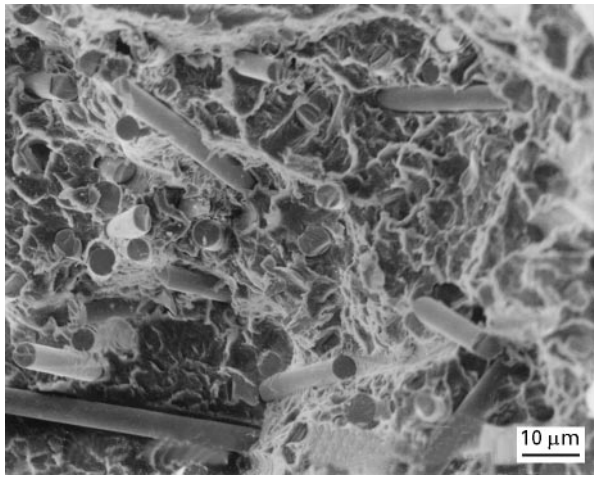


Figure 7 Fractograph of the fatigue part of the fracture surface, close to the beginning of the “crack” (dry as-moulded AL-type specimen; fatigued at 45% of UTS; lifetime, 142.862 cycles). Note the low ductility compared with the conditioned specimen (Fig. 4).

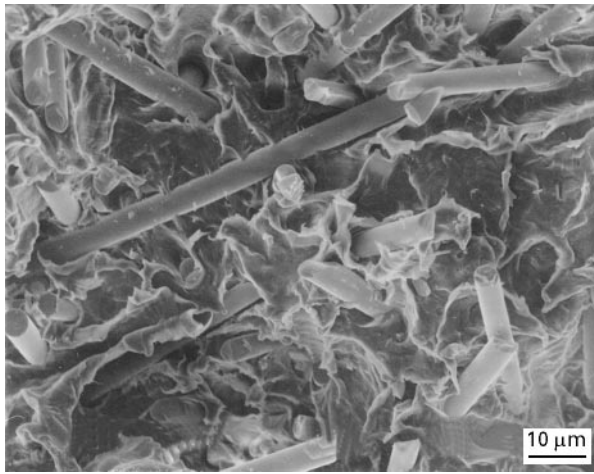


Figure 8 Fractograph of the fatigue part of the fracture surface, near the ductile-to-brittle transition. (dry as-moulded AL-type specimen; fatigued at 45% of UTS; lifetime, 142.862 cycles). The ductility is higher than at the beginning of the crack (Fig. 7).

material normally contains 1.5–2.5% water, in the PA fraction of the material. Obviously the glass cannot absorb water, but the interface between the matrix and fibre can. This leads to a permanent loss of properties of the interface, as shown by van Hartingsveldt [29]. Figs 7 and 8 show the ductile area, where the fatigue crack or damaged zone has developed. The ductility is much less than for conditioned specimens. Farther from the fibres, the matrix shows some ductility. Also the fibre–matrix bonding is much better; almost no holes around the fibres are visible. Obviously from the photographs the absorbed water has a great influence on both matrix ductility and bonding. The quality of the bonding also influences the ductility of the matrix, as a strong bond puts a high constraint on the matrix [15]. No differences in appearance of the fast fracture (brittle) part of the fracture surfaces can be seen.

Contrary to the conditioned specimens, the dry specimens show a lower ductility at the beginning of

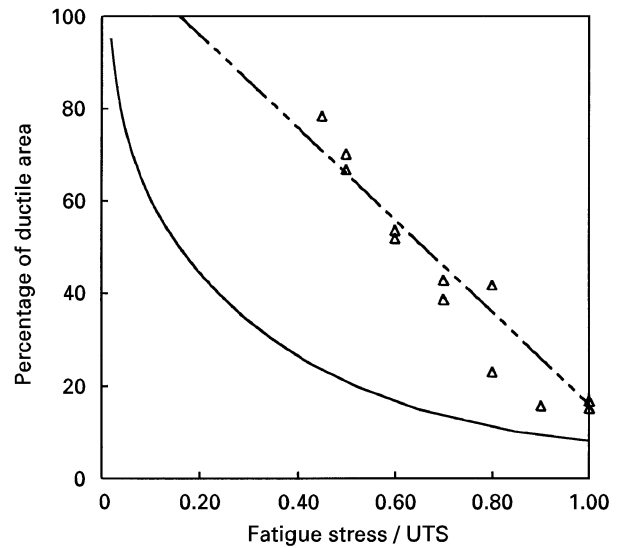


Figure 9 Ductile part of the fracture surface plotted against normalized maximum fatigue stress for conditioned specimens (Δ). (---), residual strength for the net section theory (nominal stress + 16%); (—), fracture mechanics case.

the crack. This was also seen in FCP by various researchers [23, 24]. This almost brittle fatigue surface is shown in Fig. 7. On crack growth the ductility increases slightly (Fig. 8) and then embrittles again towards the ductile–brittle transition. For the conditioned specimens this smaller ductility at the beginning of “crack” growth cannot be observed; only the decrease in ductility towards the ductile-to-brittle transition can be observed.

Comparing the dry with the conditioned specimens (Figs 7 and 4 respectively), it is seen that in the first case all fibres are broken at the fracture surface. In the second case, some fibres are pulled out of the deformed surface. In the literature this effect of broken fibres is attributed to fibre buckling during the unloading stage of the load cycle [15]. The lower ductility of the matrix and the greater constraint on the matrix through better bonding in the dry material result in a higher susceptibility of the fibres to buckling. In the conditioned material the ductility of the matrix material leaves more space for the fibres to move during unloading, leading to less fibre breakage.

4.3. Area of fatigue fracture surface

As stated above, part of the fracture surface of a fatigued specimen is microductile, and part is micro-brittle. For some specimens, both conditioned and dry as moulded, a map was made of the position of the ductile-to-brittle transition on the surface. SEM fractography had to be used for this. In Fig. 10 an example of such a map of the fracture surface is given as an inset. Damage always develops from a corner or a side of the specimen. The area of the ductile part of the fracture surface was calculated using the map. The results are presented in Figs 9 and 10, for conditioned and dry as-moulded specimens, respectively. The percentage of the fracture surface that is microductile is

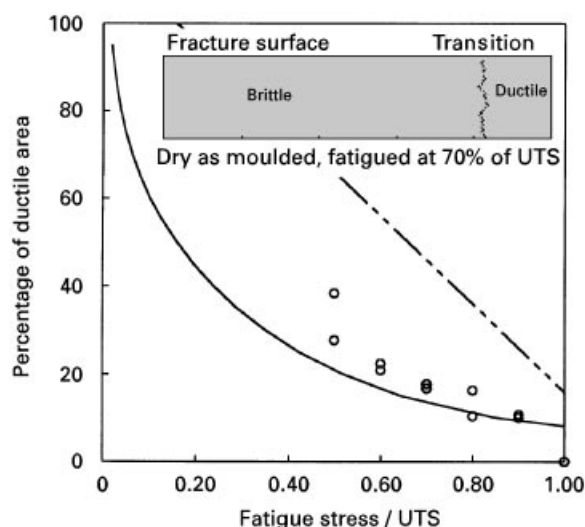


Figure 10 Ductile part of the fracture surface plotted against normalized maximum fatigue stress for dry as-moulded specimens (○). (---), residual strength for the net section theory (nominal stress + 16%); (—), fracture mechanics case.

plotted against the maximum fatigue stress, given as a percentage of UTS.

In the graphs, two lines are given for the residual strength of the specimen, assuming the ductile part of the fracture surface to be a crack. The straight line is the residual strength based on the net section; the mean net stress reaches the UTS when the crack has reached the ductile–brittle transition. The curve is based on linear fracture mechanics, considering the material to be notch sensitive. From the literature [16] a value for the critical stress intensity $K_{Ic} = 8 \text{ MPa m}^{1/2}$ was seen to be appropriate for the material under investigation. The line indicating the value where unstable crack extension would occur is based on fracture mechanics; crack extension occurs when $K_I > K_{Ic}$:

$$K_I = \sigma_{\text{nom}} Y \pi^{1/2} a \quad (1)$$

where σ_{nom} is the nominal stress, a is the crack depth (the crack is assumed to be of constant depth, over the full thickness of the specimen) and Y is a geometry factor given by

$$Y = 1.12 - 0.231 \frac{a}{w} + 10.55 \left(\frac{a}{w} \right)^2 - 21.72 \left(\frac{a}{w} \right)^3 + 30.39 \left(\frac{a}{w} \right)^4 \quad (2)$$

where w is the width of the specimen equal to (10 mm). σ_{nom} at fracture is calculated by assuming the stress intensity to be equal to the critical stress intensity: $K_I = K_{Ic}$.

The interesting result of this part of the investigation is when comparing the conditioned and dry as-moulded specimens. The measured values for the ductile percentage of the fracture surface for the conditioned specimens fit a straight line, parallel to the residual strength (straight) line for the cross-sectional area strength. This line goes through the percentage

ductile area for a tensile test (15–16% in this case). This indicates that the beginning of the final fracture is also a relatively slow process, enabling the matrix material to deform plastically. The measurements for the dry as-moulded specimens are close to the curve, for the notch-sensitive case. So the conditioned material is entirely notch insensitive, while the dry as-moulded material is notch sensitive. This result can also be interpreted in another way; the dry as-moulded fatigue damage is a real crack. In the conditioned material a bridged crack develops with fatigue. The bridges that connect both “fracture surfaces” prevent the final fast fracture until the moment when the cross-sectional area is reduced to the size where the stress in this area equals the tensile strength (UTS) of the material.

4.4. Cryogenically broken specimens

Fractography is of course very useful but has the drawback that the occurrences during fatigue may be obscured by changes that occur later in the fatigue process. To be able to observe closely not only the last events in the fracture process but also the actual occurrences during fatigue, the following method has been used to reveal the structures inside the material. Specimens were fatigued for a predetermined percentage of their expected lifetime. The fatigue lifetime can be accurately predicted using the creep speed method [6–8]. Consequently the specimens were immersed in liquid nitrogen and cryogenically broken. This way the structures caused by fatigue can be observed, because all ductile behaviour visible on the cryogenic fracture surface must be caused by the fatigue process, as the cryogenic fracture gives pure brittle behaviour.

Figs 11 and 12 show representative examples of cryogenically broken samples that were fatigued first. The samples were fatigued at 70% of the UTS for 350 cycles, approximately 90% of the expected fatigue lifetime. In Fig. 11 it is clearly seen how, although the fracture of the matrix is brittle, voids exist around the fibres. Almost no matrix material can be seen adhering to the fibres. These voids and debonding of the fibres will largely reduce their reinforcing effect, enabling the material to deform plastically in this damaged area. Increasing deformation of this damaged area will of course increase the straining of the material in front of the “craze” and will induce new voids and debonding, and growth of the “craze”.

To be able to determine the site where the damage is initiated, and where voids are formed, both fracture surfaces of one specimen were compared. Through a tedious procedure the actual voids on one surface could be traced on the other fracture surface. If on one fracture surface a void around a fibre was visible, normally the corresponding void on the other fracture surface was empty. The void was present at the fibre end. In less than 10% of the cases, both corresponding voids contained a fibre end, indicating that this was a void that was formed in the middle of the fibre. The question remains whether this fibre was broken in cryogenic fracture or during fatigue. This cannot be resolved using the current method.

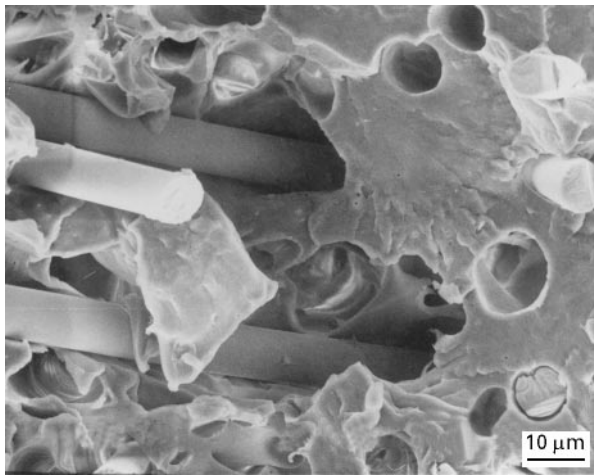


Figure 11 Representative fractograph of a cryogenically broken specimen (conditioned AL-type specimen fatigued at 70% of UTS; lifetime, 359 cycles). Voids are visible around the fibres, which cannot be caused by the cryogenic fracture, and thus must be the consequence of the fatigue process.

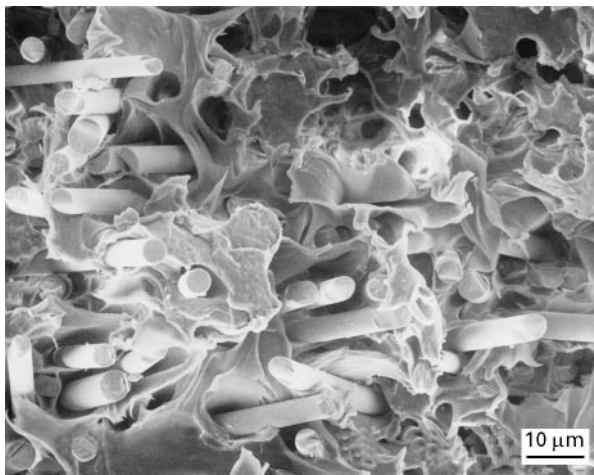


Figure 12 Small brittle fracture in a ductile area of the fracture surface of a cryogenically broken fatigued specimen (conditioned AL-type specimen; fatigued at 70% of UTS; lifetime, 359 cycles). This brittle area must have been a bridge, connecting the two “crack walls” until the final cryogenic fracture.

In Fig. 12 the damage has advanced; a small brittle part in a microductile area can be seen. This brittle part was broken cryogenically and must therefore have been a bridge that was still connecting the two crack surfaces. Theoretically it is possible that the crack was bridged also by single fibres, but this will not be visible after cryogenic fracture. This bridging fibre may break during cryogenic fracture. This cannot be distinguished from similar mechanisms that take place during fatigue. The small area broken in cryogenic fracture (in this case containing a fibre) bridges the crack, which makes it possible that the crack can still take up some load. The explanation of why this part deforms more easily than the rest of the damaged zone probably is the existing damage on levels above or below the level that we are looking at.

Figs 11 and 12 of course only give details of the damaged zone, after cryogenic fracture. We are inter-

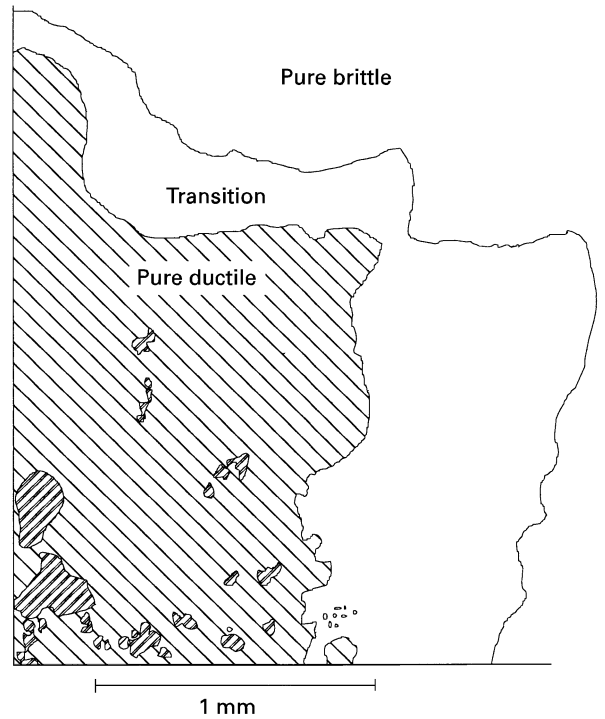


Figure 13 Map of the damaged zone of the fracture surface of a cryogenically broken fatigued specimen (conditioned AL-type specimen; fatigued at 70% of UTS; lifetime, 359 cycles). (▨), ductile; (▩), brittle.

ested in the distribution of the damage over the specimen. In Fig. 13 the corner of one cryogenically broken fatigued specimen is shown. This is the only part of the fracture surface where ductile behaviour could be observed. Close to the corner the material is entirely microductile (as in Fig. 4), except for some small zones that show microbrittle behaviour. These areas are bridges between the two crack surfaces, and obviously were present especially at the surface of the specimen, where the material can deform more easily. This is due to the lower constraint and the more random fibre orientation in the skin layer. Outside this ductile (cracked) zone a transition zone to the outer brittle zone is present. In this area, voids around the (debonded) fibres are seen, as in Fig. 11.

A final important observation is that damage could not be observed in all cryogenically broken fatigued specimens. Half the cryogenically broken specimens showed microbrittle behaviour over all the fracture surface. No ductility could be observed in these specimens although, after fatigue, stress whitening lines were visible on the specimen. Also, for the specimens where ductility was observed on the cryogenically broken fracture surface, this was observed only on a small part of the fracture surface. The damage that is the consequence of the fatigue loading is therefore confined to certain areas and is not present throughout the specimen. Combined with the fact that a number of stress whitening lines are visible on the surface, after fatigue, and the observation that on a fatigue fractured surface only part of the fracture surface is of microductile nature, the explanation for these phenomena is that damage exists in a craze-like manner.

Damage exists in zones of limited thickness, which are oriented perpendicular to the main stress direction. These zones grow in the direction of planes perpendicular to stress, during the fatigue process.

4.5. Fibre fracture phenomena

One particular phenomenon that was observed regularly, and that has not been reported before in literature, is the occurrence of fibre fracture in tension. Fibre fracture during the unloading stage due to bending or buckling [15] is reported frequently in literature. Figs 14 and 15 show two typical examples of this: a fibre end surrounded by a circular crack. The phenomenon was observed only in the ductile-to-brittle transition area, in both fatigued and tensile-tested specimens. It is a rare phenomenon; on average about 1 in 50 fibres in this transition area is broken in this way.

The reason why it is a rare phenomenon is due to the relatively short fibres. Only a very limited number of fibres are longer than the critical length. Of those fibres that are long enough for the fibre to be fully

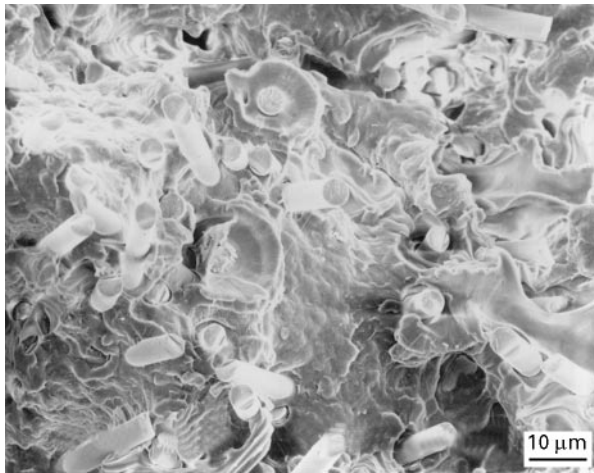


Figure 14 Broken fibres in the ductile-to-brittle transition area of a fatigued specimen.

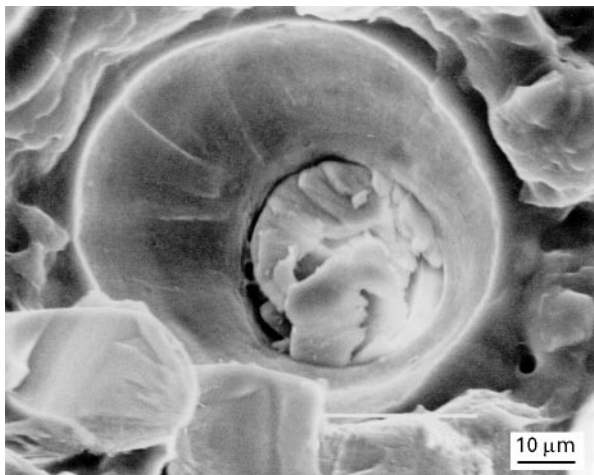


Figure 15 Detail of the broken fibre, showing the conical crack in the matrix, initiating from the fibre crack.

loaded, only a limited number have both fibre ends at a distance from the main crack, long enough for neither end to be pulled out. When looking closely at the broken fibre and surrounding crack (Fig. 15) a conical crack can be seen. The observed matrix cracks growing from a fibre fracture are very similar to those presented by ten Busschen and Selvadurai [30] and Selvadurai and ten Busschen [31]. In this pair of articles, both experimental investigations and computational modelling are compared for matrix fracture initiating at a fibre fracture in a single-fibre fragmentation test. Penny-shaped cracks, conical cracks or combinations of those were found in experiments and could also be modelled using micromechanics. The condition for these cracks to occur is a good fibre–matrix bonding; otherwise the fibre just slips through the matrix.

The reason why the material cracks is the high stress intensity, due to the presence of the very stiff fibre close to the matrix. This changes the local stress state from plane stress to plane strain. The stress intensity decreases, when going farther from the fibre. Therefore it is possible that the stress intensity drops sufficiently for the crack to stop. This is probably what we can observe in Figs 14 and 15. The material in front of the crack or damaged area is highly strained, high enough for a long fibre in this area to break. At this moment the matrix in this area is still intact. On fracture of the fibre a very high stress intensity in the matrix exists and causes a crack to initiate and grow, from the fibre fracture. When the crack grows, the stress intensity lowers, and the crack stops growing. This pattern is consequently revealed when the main crack grows and surpasses this circular crack. The similarity between the patterns found here and those in [30, 31] for single-fibre specimens with a polyester resin matrix is quite surprising, taking into account the different circumstances. In Fig. 14 it can be seen that the crack around the fibre is not always completely circular, depending on the presence of other fibres.

5. Conclusions

A fatigue failure mechanism of bridged cracks as presented in [6, 7] could be proven. The mechanism is visualized in Fig. 16, numbers in the figure are explained here. Damage is initiated at the location of highest stress intensity, the fibre ends, 1. Fibre ends are badly bonded to the matrix, because no coating is present. This because the fibres are broken during compounding and injection moulding. Voids grow from this damage, along the fibres, 2. In a small percentage of cases, voids develop in the middle of a fibre, or at a fractured fibre. These voids grow, 3, and coalesce, 4, but no complete crack will develop. Both “crack” walls remain connected by bridges, which occur mainly at the specimen surface. The method of cryogenically breaking fatigued specimens was very successful in revealing the structure of damage in a fatigued specimen and clarifying the fatigue mechanism. The failure mechanism as was found in these investigations may exist in SFRTs with different

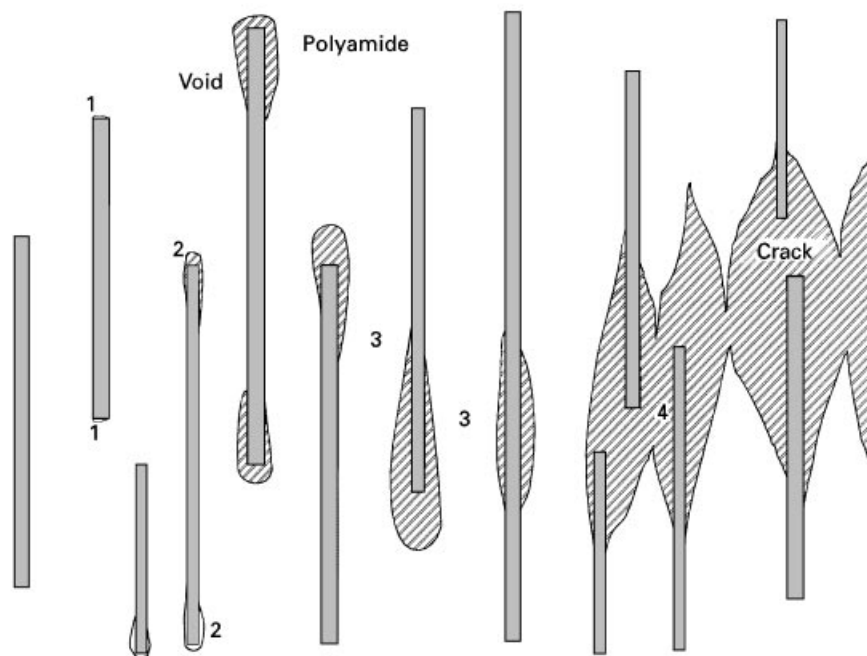


Figure 16 Visualization of the failure mechanism in an idealized reinforced system. The numbers are explained in the text.

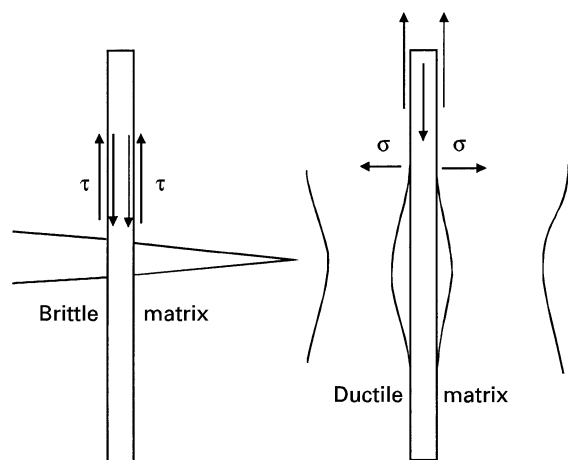


Figure 17 Fibre-matrix interface loading: (a) tensile; (b) fatigue.

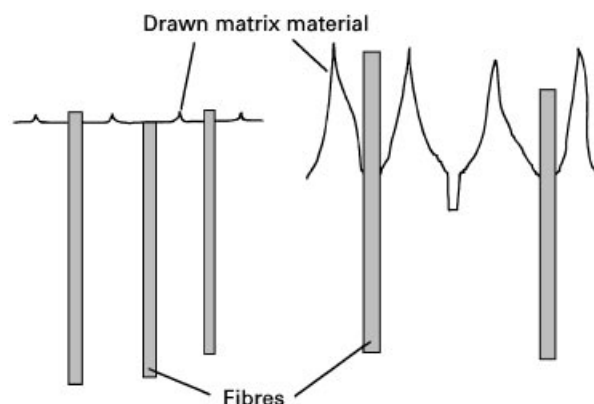


Figure 18 Difference in mechanism between (a) conditioned and (b) dry as-moulded material. The higher ductility in the former case may not be solely caused by the higher ductility of the matrix. Also the lower constraint on the matrix, due to weaker bonding, may cause this.

matrix materials as well, provided that this matrix possesses the necessary ductility.

The differences between the fracture surfaces in fatigue experiments and tensile tests that were found in these experiments were similar to those found in the literature (Section 2). The possible cause for the difference between the fibre-matrix bondings in the two cases is the difference between the matrix ductilities. In fatigue the local stress intensity at the fibre ends is high; damage will occur. Debonding in a shear mode will take place at the ends of the fibres, where the shear stress at the interface is the highest. Unloading of the fibres due to debonding will increase the local stress on the matrix, which will deform. Deformation of the matrix requires lateral contraction, which is inhibited by the bonding to the surrounding fibres. This results in a tensile stress on the fibre-matrix interface. Thus, for fatigue behaviour, not just the pull-out (shear) strength of the interface but also its tensile strength are

of importance. This is the main difference between fatigue and tensile experiments (Fig. 17). In tensile experiments the matrix cracks in a brittle manner. Loading of the fibre therefore is in pure shear, because lateral contraction of the matrix is absent. Under this shear stress the interface itself does not fail (in well-bonded systems); the matrix close to the interface fails. This is shown by the matrix material that is seen adhering to the pulled-out fibres.

Obviously the tensile stress on the interface that does occur in fatigue makes the interface itself fail. This is seen in the fibres with no matrix material adhering to them.

Many differences between fractography and failure mechanisms in fatigue reported by different researchers can be attributed to differences between either ductilities and/or fibre-matrix bondings. In investigations where PA has been used, these differences

can be caused by different conditioning treatments of the specimens. Specimens that have been conditioned to equilibrium water content will have matrix material with a much more ductile behaviour, compared with specimens investigated in their dry as-moulded state. In both cases, ductility is present, although in the conditioned state this is much more pronounced. A comparison has been visualized in Fig. 18, for a model system. The difference in ductility is enhanced by the detrimental effect of water on the fibre-matrix interface strength. Consequently a lower constraint on the matrix gives an apparently higher ductility in the conditioned case.

References

1. M. AKAY and D. BARKLEY, *J. Mater. Sci.* **26** (1991) 2731.
2. T. MATSUOKA, J. I. TAKABATAKE, Y. INOUE and H. TAKAHASI, *Polym. Engng. Sci.* **30** (1990) 957.
3. M. G. WYZGOSKI and G. E. NOVAK, *Polym. Preprints, Amer. Chem. Soc.* **29** (1988) 132.
4. D. McNALLY, *Polym. Plast. Technol. Engng.* **8** (1977) 101.
5. M. AKAY and D. F. O'REGAN, *Plast. Rubber Comp. Proc. Appl.* **24** (1995) 97.
6. J. J. HORST and J. L. SPOORMAKER, *Polym. Engng. Sci.* **36** (1996) pp. 2718–26.
7. J. J. HORST, in "Proceedings of the Third International Conference on Deformation and Fracture of Composites," Surrey, March 1995 (Institute of Metals, London, 1995) p. 473.
8. J. J. HORST, in "Proceedings of the Tenth Biennial European Conference on Fracture, Berlin, September 1994, edited by K.-H. Schwalbe and C. Berger (Engineering Materials Advisory Services Ltd, Warley, 1994) p. 1187.
9. J. J. HORST, in "Proceedings of the 11th Biennial European Conference on Fracture", ed. J. Petit, EMAS, Warley, UK, Poitiers, September 1996 (1996) 1057–62.
10. B. D. AGARWAL and L. J. BROUTMAN, in "Analysis and performance of fiber composites" (Wiley, New York, 1990).
11. M. J. FOLKES, in "Short fibre reinforced thermoplastics" (Research Studies Press, Wiley, New York, 1982).
12. K. L. JERINA, J. C. HALPIN and L. NICOLAIS, *Ing. Chim. Ital.* **9** (1973) 94.
13. M. R. PIGGOTT, in "Load bearing fibre composites" (Pergamon, Oxford, 1980).
14. N. SATO, S. SATO and T. KURAUCHI, in "Proceedings of the Fourth International Conference on Composite Materials, Tokyo, October 1982 (Japan Society for Composite Materials, Tokyo, 1982) 1061–66.
15. R. W. LANG, J. A. MANSON and R. W. HERTZBERG, *J. Mater. Sci.* **22** (1987) 4015.
16. J. C. MALZAHN and K. FRIEDRICH, *J. Mater. Sci. Lett.* **3** (1984) 861.
17. R. W. HERTZBERG and J. A. MANSON, in "Fatigue of engineering plastics" (Academic Press, New York, 1980).
18. J. W. DALLY and D. H. CARRILLO, *Polym. Engng. Sci.* **9** (1969) 433.
19. J. F. MANDELL, F. J. MCGARRY and C. G. LI, Department of Materials Science and Engineering, Massachusetts Institute of Technology, Cambridge, Research Report R83-1 (1983).
20. A. T. DIBENEDETTO and G. SALEE, *Polym. Engng. Sci.* **19** (1979) 512.
21. N. SATO, T. KURAUCHI, S. SATO and O. KAMIGAITO, *J. Mater. Sci.* **26** (1991) 3891.
22. J. KARGER-KOCSIS and K. FRIEDRICH, *Composites* **19** (1988) 105.
23. V. M. KARBHARI and A. DOLGOPOLSKY, *Int. J. Fatigue* **12** (1990) 51.
24. J. KARGER-KOCSIS, *Composites* **21** (1990) 243.
25. J. KARGER-KOCSIS and K. FRIEDRICH, *ibid.* **19** (1988) 105.
26. H. VOSS and J. KARGER-KOCSIS, *Int. J. Fatigue* **10** (1988) 3.
27. J. F. MANDELL, D. D. HUANG, F. J. MCGARRY, in "Preprints of the 35th Annual Conference of the Reinforced Plastics/Composites Institute", New Orleans, LA, 1980 (1980) Preprint 20-D.
28. R. W. LANG, J. A. MANSON and R. W. HERTZBERG, *Org. Coatings Plast. Chem.* **45** (1981) 778.
29. E. A. A. VAN HARTINGSVELDT, PhD thesis, Delft (1987).
30. A. TEN BUSSCHEN and A. P. S. SELVADURAI, *J. Appl. Mech.* **62** (1995) 87.
31. A. P. S. SELVADURAI and A. TEN BUSSCHEN, *ibid.* **62** (1995) 98.

Received 13 May 1996
and accepted 20 January 1997